Volume 7 | Number 7 | 7 April 2017 | Pages 1451–1613

Catalysis Science & Technology

rsc.li/catalysis

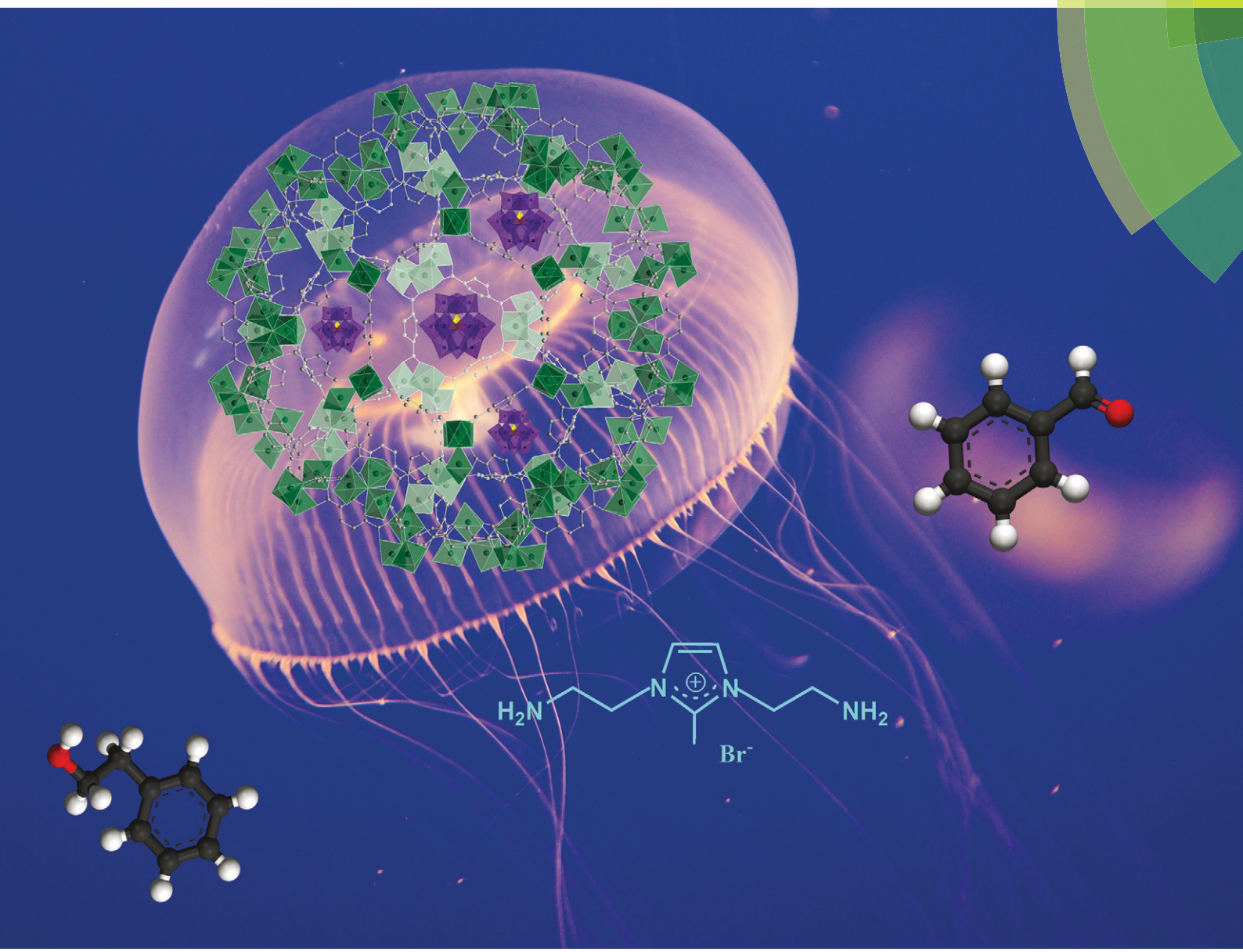

ISSN 2044-4761

ROYAL SOCIETY OF CHEMISTRY

PAPER

Pascal Van Der Voort *et al.*

POM@IL-MOFs – inclusion of POMs in ionic liquid modified MOFs to produce recyclable oxidation catalysts

Catalysis Science & Technology

PAPER

Cite this: *Catal. Sci. Technol.*, 2017, 7, 1478

POM@IL-MOFs – inclusion of POMs in ionic liquid modified MOFs to produce recyclable oxidation catalysts†

Sara Abednatanzi,[ab] Karen Leus,[a] Parviz Gohari Derakhshandeh,[bc] Fady Nahra,[c] Katrien De Keukeleere,[c] Kristof Van Hecke,[c] Isabel Van Driessche,[c] Alireza Abbasi,[b] Steven P. Nolan[cd] and Pascal Van Der Voort*[a]

Received 22nd December 2016,
Accepted 6th February 2017

DOI: 10.1039/c6cy02662a

rsc.li/catalysis

In this study, we present for the first time the immobilization of phosphotungstic acid ($H_3PW_{12}O_{40}$, HPW) into the nanocages of a dual amino-functionalized ionic liquid (DAIL)-modified MIL-101(Cr) framework under mild conditions. The obtained PW/DAIL/MIL-101(Cr) was evaluated as a catalyst in the oxidation of benzyl alcohol using TBHP in chloroform. In order to obtain insights into the role of the DAIL during catalysis, a DAIL-free catalyst (HPW/MIL-101(Cr)) was also prepared. Both catalysts were fully characterized using several techniques. In comparison with the HPW/MIL-101(Cr) material, PW/DAIL/MIL-101(Cr) showed an enhanced catalytic performance in the selective oxidation of benzyl alcohol. This was mainly attributed to the ability of the DAIL groups to form hydrogen bonds, thus enhancing the accessibility of TBHP. Furthermore, the immobilization of the DAIL groups onto MIL-101(Cr) resulted in increased thermal stability of the obtained PW/DAIL/MIL-101(Cr) which showed stability up to 400 °C. Moreover, the PW/DAIL/MIL-101(Cr) catalyst exhibited good recyclability and selectivity. The catalyst could be reused for at least five cycles with no significant leaching of the tungsten species or loss of crystallinity and activity.

1 Introduction

Selective oxidation of primary alcohols to aldehydes is one of the most sought-after transformations since aldehydes are highly important targets in both academia and industry.[1–4] From an industrial point of view, one of the significant challenges in such oxidation is to avoid the over-oxidation of aldehydes into acids, as selectivity targeting the sole production of aldehydes would impact processes where aldehydes act as intermediates in the synthesis of pharmaceutical and agrochemical compounds.[5,6]

Polyoxometalates (POMs), a class of structurally diverse anionic transition metal oxide clusters, have already been shown to be promising catalysts for a number of oxidation reactions, owing to their redox and acid properties.[7–10] Moreover, with this type of chemistry, incorporation of organic units into POM anions has received considerable interest as an efficient approach to develop POM-derived materials.[11] Within this context, functionalized organic ionic liquid (IL) cations have been demonstrated to be among the most effective modifiers for POMs by increasing the catalytic activity of the latter in selective oxidation reactions.[12–15]

Despite these interesting features of POM-based ILs and recent advances in the design and synthesis of these highly active catalysts, clean separation and recycling still pose a considerable challenge.[16–18] Therefore, for practical applications, it is of paramount importance to immobilize the catalytically active POM-based ILs onto appropriate solid supports which combine the attractive features of POM-based ILs with the benefits of heterogeneous catalysis.[19]

Metal–organic frameworks (MOFs) constitute an emerging class of porous materials due to their thermal and chemical stabilities and large surface areas; they possess regular and accessible pores that make them outstanding candidates to act as a support for various active centres.[20–22] Many attempts have been made to insert catalytically active molecules into the nanocages of MOFs *via* a post-synthetic strategy.[23–27] Within this context, the mesoporous chromium terephthalate, denoted as MIL-101(Cr), has been the most examined host material for the immobilization of catalytic species.[28–32]

[a] *Department of Inorganic and Physical Chemistry, Center for Ordered Materials, Organometallics and Catalysis (COMOC), Ghent University, Krijgslaan 281-S3, 9000 Ghent, Belgium. E-mail: Pascal.VanDerVoort@UGent.be*
[b] *School of Chemistry, College of Science, University of Tehran, P.O. Box 14155-6455, Tehran, Iran*
[c] *Department of Inorganic and Physical Chemistry, Ghent University, Krijgslaan 281-S3, 9000 Ghent, Belgium*
[d] *Chemistry Department, College of Science, King Saud University, PO Box 2455, Riyadh, 11451, Saudi Arabia*

† Electronic supplementary information (ESI) available: Characterization of HPW/MIL-101(Cr), textural properties and elemental analysis of PW/DAIL/MIL-101(Cr) materials, characterization of the recycled PW/DAIL/MIL-101(Cr). See DOI: 10.1039/c6cy02662a

The large surface area with accessible mesoporous cages and high thermal and chemical stabilities make this MOF an attractive solid support.[33,34]

Although there are some reports about the preparation of POM-based IL hybrid materials using mesoporous silica and magnetic nanoparticles,[35–40] to the best of our knowledge, there is only one report on the utilization of ILs using MOFs as a solid support for the immobilization of POMs.[41] In the latter case, a heteropolyanion-based IL was encapsulated within the framework of MIL-100. The prepared catalyst exhibited an enhanced catalytic performance in the esterification of oleic acid in comparison with the encapsulated heteropolyanion within the framework. The presence of a sulfonic acid group-functionalized IL led to an increased number of acid sites, which resulted in a higher catalytic activity of the prepared material.[41]

It is interesting to note that immobilization of POMs onto MOFs using a post-synthetic strategy is challenging, as most POM-loaded MOFs reported so far lack sufficient thermal and chemical stabilities to prevent leaching of the active components.[30] As a consequence, there is a strong need to develop new POM–MOF stable catalysts. For the first time, we report on the utilization of a supported dual amino-functionalized ionic liquid (DAIL) in designing a new and efficient POM-based oxidation catalyst using MIL-101(Cr) as a support. For this purpose, MIL-101(Cr) was synthesized in water under HF-free conditions. The coordinatively unsaturated chromium sites (CUS) present in the MIL-101(Cr) structure are used as anchoring points for the immobilization of the IL through a post-synthetic strategy. In addition, the supported dual amino-functionalized ionic liquid was used for the immobilization of the Keggin-type $H_3PW_{12}O_{40}$ (HPW) inside the nanocages of MIL-101(Cr) through anion exchange. The HPW can easily diffuse into the pores of MIL-101(Cr) and react with the DAIL groups to form a POM-based IL. The remaining free amino groups in the DAIL play an important role in enhancing the accessibility of TBHP through the formation of hydrogen bonds which results in an increased catalytic performance. The catalytic activity of the prepared PW/DAIL/MIL-101(Cr) material was examined in the selective oxidation of benzyl alcohol.

2 Experimental

2.1. Catalyst characterization

All reagents were purchased from Sigma-Aldrich or TCI Europe and used without further purification.

Diffuse reflectance infrared Fourier transform spectroscopy (DRIFTS) measurements were obtained using a Thermo Nicolet 6700 FT-IR spectrometer equipped with a nitrogen-cooled MCT-A (mercury–cadmium–tellurium) detector and a KBr beam splitter. Powder X-ray diffraction (PXRD) patterns were recorded on a Thermo Scientific ARL X'Tra diffractometer, operated at 40 kV and 40 mA using Cu-Kα radiation (λ = 1.5406 Å).

The surface area and pore volume of the samples were determined by nitrogen adsorption/desorption measurements at liquid nitrogen temperature using a Belsorp-mini II gas analyzer. Before the adsorption experiments, the samples were degassed under vacuum at 90 °C for 24 h. Thermogravimetric analysis (TGA) was performed using a NET-ZSCH STA 409 PC/PGTG instrument. The samples were heated from 30 to 800 °C in air at a constant rate of 10 °C min^{-1}. An ultra-fast GC equipped with a flame ionization detector (FID) and a 5% diphenyl/95% polydimethylsiloxane column with a 10 m length and a 0.10 mm internal diameter was used to monitor the conversion of the products during the catalytic tests. Helium was used as the carrier gas and the flow rate was programmed to be 0.8 mL min^{-1}. The reaction products were identified using a TRACE GC × GC (Thermo, Interscience) coupled to a TEMPUS TOFMS detector (Thermo, Interscience). The first column consists of a dimethyl polysiloxane package and has a length of 50 m with an internal diameter of 0.25 mm, whereas the second column has a length of 2 m with an internal diameter of 0.15 mm. The package of the latter is 50% phenyl polysilphenylene-siloxane. Helium was used as the carrier gas with a constant flow (1.8 mL min^{-1}).

^{1}H NMR spectra are recorded in D_2O on a Bruker 300 MHz AVANCE spectrometer with chemical shifts (δ) expressed in ppm relative to a tetramethylsilane standard. Elemental analyses were performed using an ICP-OES Optima 8000 (inductively coupled plasma optical emission spectroscopy) atomic emission spectrometer. X-ray fluorescence (XRF) measurements were carried out by means of a NEX CG from Rigaku using a Mo X-ray source. The nitrogen content of the modified materials was determined using a Thermo Flash 200 elemental analyzer with V_2O_5 as a catalyst. Transmission electron microscopy (TEM) and high angular annular dark field scanning transmission electron microscopy (HAADF STEM) images were obtained using a JEOL JEM-2200FS transmission electron microscope with a post-sample Cs corrector and an accelerating voltage of 200 kV. For the sample preparation, the powder was dispersed in methanol and treated ultrasonically for 2 minutes. A copper support TEM grid (200 mesh) is dipped in the dispersion and air-dried before measurement.

2.2. Catalyst preparation

2.2.1. Synthesis of the dual amino-functionalized ionic liquid 1,3-di(2′-aminoethyl)-2-methylimidazolium bromide (DAIL). The dual amino-functionalized ionic liquid was synthesized according to a previously reported procedure[42] and is depicted in Scheme 1. The successful synthesis of the material was confirmed by ^{1}H NMR spectroscopy.

2.2.2. Preparation of the supported DAIL (DAIL/MIL-101(Cr)). The MIL-101(Cr) sample was prepared under HF-free conditions according to a slightly modified procedure described by Edler *et al.*[43] Typically, 0.6645 g of terephthalic acid was mixed with 1.6084 g of $Cr(NO_3)_3{\cdot}9H_2O$ and 20 mL of distilled water. The mixture was transferred into a Teflon-

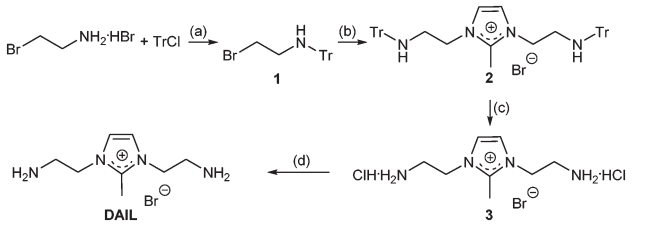

Scheme 1 Synthetic route to DAIL. (a) Et_3N, CH_2Cl_2, room temp., 24 h; (b) 2-methylimidazole and NaH (60%), DMF, reflux, 8 h; (c) HCl, CH_3OH, room temp., 24 h; (d) NaOH, H_2O, room temp., 3 h.

lined autoclave, sealed, and then heated for 2 h to 210 °C at which it was held for 8 h. After cooling to room temperature, the MIL-101(Cr) was filtered, washed with acetone, and stirred in dimethylformamide for 24 h to remove any unreacted terephthalic acid. Thereafter, the MIL-101(Cr) was filtered and dried under vacuum at 90 °C overnight. The dehydrated form of MIL-101(Cr) was obtained by heating the pristine material at 150 °C under vacuum for 24 h to generate open metal centers. The immobilization of the DAIL was achieved by the addition of MIL-101(Cr) (150 mg) to a solution of DAIL (0.3, 0.6, 0.9, 1.5 mmol g^{-1}) in 2.5 mL ethanol. The mixture was stirred at room temperature for 24 h. The resulting solid was collected by filtration and washed several times with ethanol. Then, the resulting solid was dried under vacuum overnight.

2.2.3. Preparation of immobilized PW onto the supported DAIL (PW/DAIL/MIL-101(Cr)). The PW/DAIL/MIL-101(Cr) sample was prepared by adding DAIL/MIL-101(Cr) (150 mg) to a solution of HPW in acetonitrile (0.23 mmol g^{-1}, 2.5 ml). The mixture was stirred at ambient temperature for 24 h. Afterwards, the catalyst was collected by filtration, washed several times with acetonitrile (3 × 20 ml) and dried under vacuum for 24 h.

2.2.4. Preparation of immobilized HPW onto MIL-101(Cr) (HPW/MIL-101(Cr)). MIL-101(Cr) (150 mg) was suspended in a solution of HPW in acetonitrile (0.227 mmol g^{-1}, 2.5 ml) and the mixture was stirred at ambient temperature for 24 h. The solid was collected by filtration and washed several times with acetonitrile (3 × 20 ml).

2.3. General procedure for the oxidation of benzyl alcohol

During a typical catalytic test, PW/DAIL/MIL-101(Cr) (6 μmol based on W), *tert*-butyl hydroperoxide (TBHP, 5-6 M in decane, 4.5 mmol), dodecane as an internal standard (0.5 mmol), benzyl alcohol (1 mmol) and chloroform (1 ml) were added into a Schlenk tube. The tube was sealed and then heated to 100 °C for 6 h. The PW/DAIL/MIL-101(Cr) material was activated under vacuum at 90 °C prior to catalysis. After each catalytic run, the catalyst was recovered by filtration, washed with chloroform and used directly in the subsequent runs. Samples were withdrawn after 6 h reaction, and after cooling and dilution with the solvent, were analyzed using an ultra-fast gas chromatograph (Thermo, Interscience) equipped with a flame ionization detector (FID).

3 Results and discussion

3.1. Preparation and structural information of immobilized PW onto the supported DAIL (PW/DAIL/MIL-101(Cr))

MIL-101(Cr), a three-dimensional chromium(III) terephthalate MOF, possesses regular mesoporous cages of 29 and 34 Å, which are accessible through windows of *ca.* 12 and 16 Å.[33] Interestingly, the existence of coordinatively unsaturated chromium sites (CUSs) in the framework provides opportunities for the incorporation of active species. In this regard, the treatment of the activated MIL-101(Cr) with the prepared DAIL afforded DAIL/MIL-101(Cr), as there is strong coordination between the metal centres and the amino groups of the supported DAIL. In the following, the immobilization of PW onto the supported DAIL was performed through anion exchange of the corresponding cluster and the DAIL. The PW cluster, with dimensions of about 12 Å, has the appropriate size to diffuse through the larger windows of the framework. A schematic illustration for the preparation of the catalyst is outlined in Scheme 2.

3.2. Characterization of immobilized PW onto the supported DAIL (PW/DAIL/MIL-101(Cr))

3.2.1. X-ray diffraction, nitrogen adsorption and thermogravimetric analysis. In Fig. 1, the PXRD patterns of MIL-101(Cr) and the post-modified materials are presented. The pattern of the pristine MIL-101(Cr) corresponds well with the simulated one, indicating the phase purity of MIL-101(Cr) under the applied synthesis conditions. However, the observed broadening in the PXRD patterns of the as-synthesized MIL-101(Cr) (MIL-101(Cr) before modification) is due to the fact that the resulting product consisted of crystals having various sizes, as supported by TEM images. Moreover, the PXRD patterns revealed a shift for all peaks to higher 2θ angles. This behavior might be due to the shrinkage of the framework depending on the removal of guest molecules

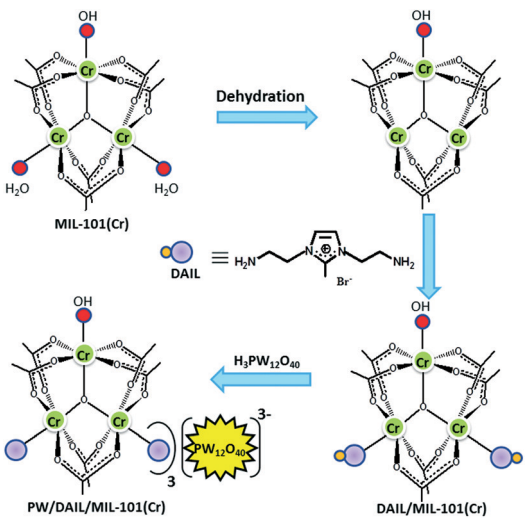

Scheme 2 Schematic illustration for the preparation of PW/DAIL/MIL-101(Cr).

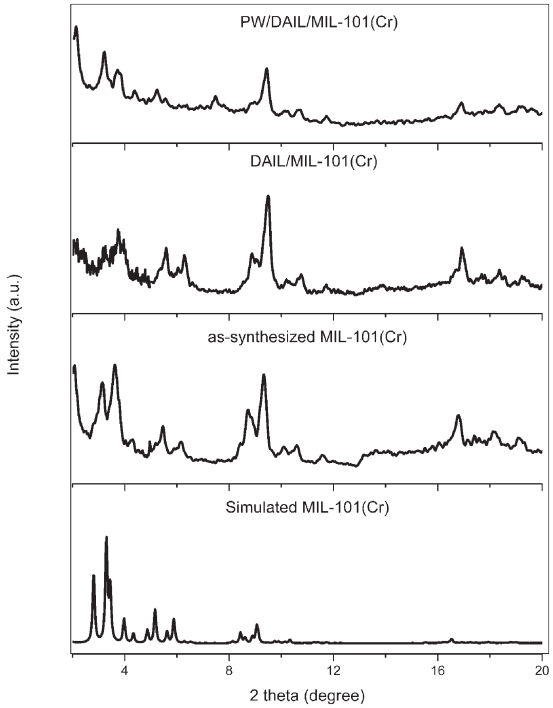

Fig. 1 XRD patterns of MIL-101(Cr) and the modified materials.

inside the pores after drying under vacuum at 90 °C. A similar broadening to the parent MIL-101(Cr) was observed for the isoreticular NH_2-MIL-101(Cr).[28] The PXRD pattern of the functionalized MIL-101(Cr) with the DAIL groups is in good accordance with that of the parent MIL-101(Cr), which implies that the crystal structure remained intact after the introduction of the DAIL groups. In the PXRD pattern of the PW/DAIL/MIL-101(Cr) catalyst, one can see that all the main diffraction peaks are present, however, some variations in the relative intensity of the diffraction peaks are observed. Similar observations were reported previously for the modified POM-MILs due to the interaction of the clusters with the MIL-101(Cr) or changes in the symmetry of the clusters within the nanocages of the framework.[44]

Nitrogen adsorption/desorption experiments were performed to evaluate the porosity of the pristine and modified samples. Fig. 2 shows the N_2 adsorption/desorption isotherms of MIL-101(Cr) and the modified materials. The pristine MIL-101(Cr) exhibits secondary uptakes at about p/p_0 = 0.1 and p/p_0 = 0.2, which indicates the presence of two nanoporous windows.[45] The Langmuir surface area and total pore volume for the prepared MIL-101(Cr) are 3735 $m^2\ g^{-1}$ and 1.48 $cm^3\ g^{-1}$, respectively. Compared with the pristine MIL-101(Cr), the DAIL-modified sample shows a decrease in both the Langmuir surface area and pore volume (3049 $m^2\ g^{-1}$ and 1.41 $cm^3\ g^{-1}$, respectively) owing to the insertion of the DAIL groups into the nanocages of the framework. However, the modified sample still possesses a large surface area to provide sufficient space for the introduction of PW POM. As expected, the PW/DAIL(0.3)/MIL-101(Cr) material shows an additional decrease in the Langmuir surface area

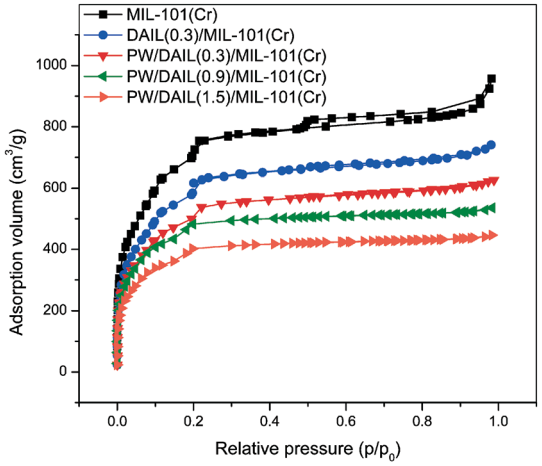

Fig. 2 Nitrogen sorption isotherms of MIL-101(Cr) and the modified materials.

and pore volume (2704 $m^2\ g^{-1}$ and 1.35 $cm^3\ g^{-1}$, respectively) compared to the DAIL/MIL-101(Cr) sample, which is a clear indication of the successful immobilization of PW inside the framework. The textural properties and elemental analysis of all the samples are listed in Table S1.†

Thermal analysis was performed to monitor the decomposition profiles of the pristine MIL-101(Cr), DAIL/MIL-101(Cr) and PW/DAIL/MIL-101(Cr) catalyst. The obtained results are depicted in Fig. 3. The presence of the DAIL and PW molecules in MIL-101(Cr) was also confirmed by means of TGA. In the TGA profile of the pristine MIL-101(Cr), three distinct weight loss steps can be observed: the first weight loss (between 25–150 °C) corresponds to the loss of guest water and organic solvent molecules. With the further increase in temperature, the removal of chemically bonded water occurs. In the third step (between 325–470 °C), the weight loss of approximately 57% is attributed to the elimination of OH groups and the framework decomposition. The TGA curves for the DAIL/MIL-101(Cr) and PW/DAIL/MIL-101(Cr) materials are similar to that of the pristine MIL-101(Cr), albeit the initial weight loss up to 150 °C is less pronounced since the

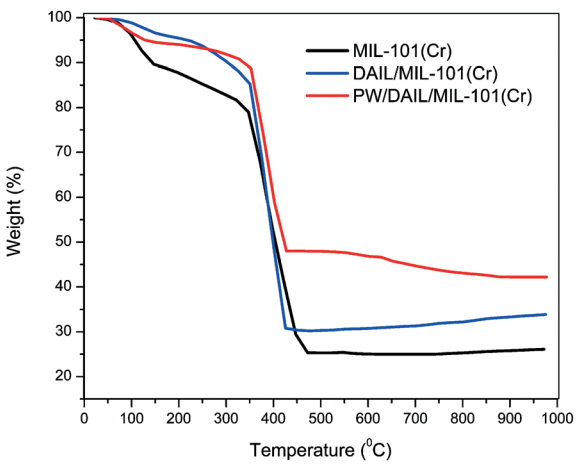

Fig. 3 TGA curves of MIL-101(Cr) and the modified materials.

cages of MIL-101(Cr) were occupied by the DAIL and PW. The TGA curve of DAIL/MIL-101(Cr) indicates a weight loss at 250–380 °C, which is probably due to the decomposition of the DAIL inside the pores. In contrast to the latter material, PW/DAIL/MIL-101(Cr) shows good thermal stability at these temperatures.

The enhanced thermal stability of PW/DAIL/MIL-101(Cr) compared to DAIL/MIL-101(Cr) may be due to the additional interactions between DAIL and PW molecules. After 600 °C, a shoulder can be seen in the TGA curve, which is ascribed to the decomposition of the PW POM.

3.2.2. Spectroscopic analysis. DRIFT measurements were performed to gain insight into the structural features of the pristine and functionalized samples. The DRIFT spectra of all the samples are presented in Fig. 4. In the DRIFT spectrum of the DAIL, the characteristic peaks of the imidazole fragment appear at 1590 and 1668 cm^{-1} which can be assigned to the vibrations of the C═C and C═N groups.[46] The bands at 1111, 1160 and 2953 cm^{-1} can be ascribed to the C–N, C–C and C–H stretching vibrations of the alkyl chain.[46] These vibrations can also be seen in the DRIFT spectrum of the DAIL/MIL-101(Cr) sample, which clearly confirms the successful attachment of the DAIL to the free metal sites. As shown in Fig. 4, the characteristic bands at approximately 1080, 979 and 900 cm^{-1}, which appeared in the DRIFT spectrum of the supported PW/DAIL/MIL-101(Cr), can be assigned to the vibrations of P–O, W═O and W–O–W in the POM, respectively.[44] These DRIFT results demonstrate that PW molecules have been successfully deposited onto DAIL/MIL-101(Cr).

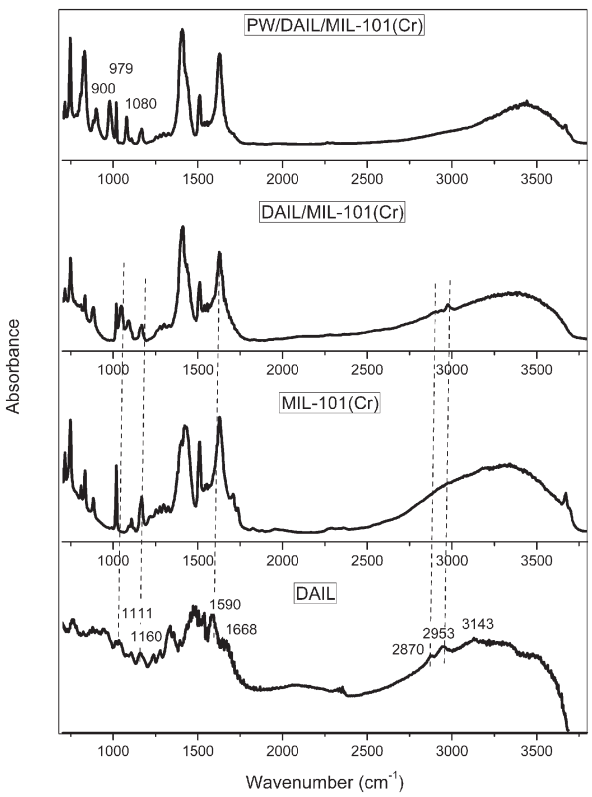

Fig. 4 DRIFT spectra of MIL-101(Cr) and the modified materials.

3.2.3. Transmission electron microscopy measurements. In order to investigate the morphology and composition of the PW/DAIL/MIL-101(Cr) material, TEM, STEM and elemental mapping were conducted. Fig. 5a shows a dark-field STEM micrograph of the modified MIL-101(Cr) compound demonstrating a typical truncated octahedral morphology. Moreover, the material shows perfect TEM images of the pore distribution within the crystals (Fig. 5c and d). These observations confirm that the morphology of the support was preserved after the modification process. Interesting features could be observed from both TEM and elemental mapping images. The TEM images in Fig. 5c and d show places with darker contrast that could be assigned to the presence of polyoxometalate molecules inside the MIL-101(Cr) cavities and not on the external surface. Elemental mapping (Fig. 6) further revealed the elements, including W, P and Cr, from both polyoxometalates and MIL-101(Cr). In addition, this image displays a very nice and homogeneous distribution of polyoxometalates in the MIL-101(Cr) material.

3.3. Catalytic tests

The catalytic activity of the obtained PW/DAIL/MIL-101(Cr) material was evaluated in the selective oxidation of benzyl alcohol to benzaldehyde using TBHP as the oxidant. The surface area, as well as the distribution of the active sites within the porous support, plays an important role in the catalytic reaction. In this case, MIL-101(Cr) as the solid support provides a high surface area even after the immobilization of the PW molecules, which further allows the facile diffusion of the reactants within the framework. In order to obtain insights into the function of the DAIL moiety, the DAIL-free catalyst (HPW/MIL-101(Cr)) was synthesized through the impregnation of MIL-101(Cr) with HPW POM using the original reaction

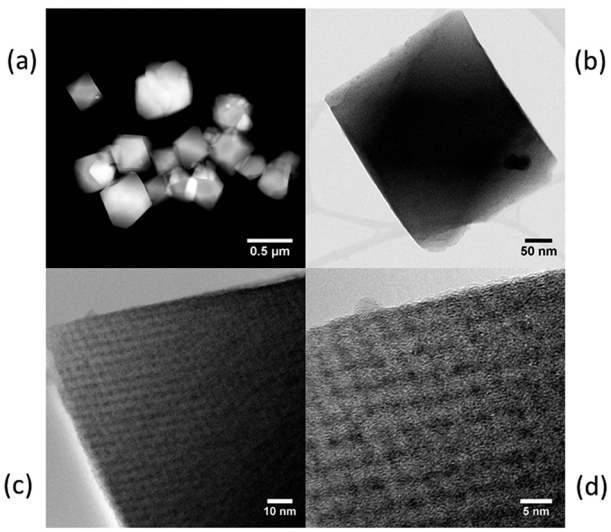

Fig. 5 (a) Dark-field STEM image, (b) bright-field STEM image, (c) and (d) TEM images of PW/DAIL/MIL-101(Cr).

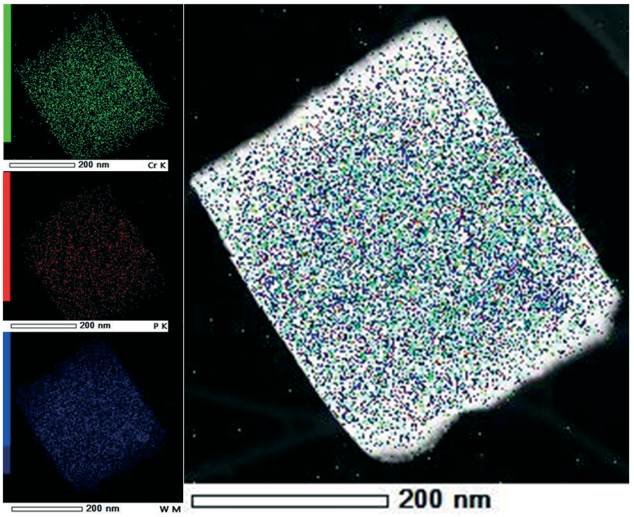

Fig. 6 EDX elemental mapping images for the PW/DAIL/MIL-101(Cr) material.

conditions of the PW/DAIL/MIL-101(Cr) catalyst. HPW/MIL-101(Cr) was fully characterized (see Fig. S1–S4†). The W loading was determined by means of XRF measurements, indicating a loading of 0.18 mmol g^{-1} and 0.23 mmol g^{-1} for the HPW/MIL-101(Cr) and the PW/DAIL/MIL-101(Cr) materials, respectively. The slightly higher metal loading in the PW/DAIL/MIL-101(Cr) catalyst may be due to less significant PW leaching into the liquid environment, which arises from the additional interactions between DAIL and PW molecules.

In a typical catalytic test, a catalyst loading of 6 μmol W was used and the substrate/oxidant ratio was 1 : 4.5 (mmol). The results of the catalytic performance of the PW/DAIL/MIL-101(Cr) material are given in Table 1.

As mentioned above, the selective oxidation of alcohols to aldehydes and ketones without forming over-oxidized products is of great importance.[5,6] These over-oxidation reactions occur due to the large activation energy required to bring about the first step in the oxidation reaction.[47] In all the cases examined in this study, complete selectivity towards the formation of benzaldehyde is obtained (>99%), demonstrating that the POM-based catalyst exhibits excellent product selectivity under the reaction conditions. PW/DAIL/MIL-101(Cr) exhibits a higher catalytic performance in the oxidation of benzyl alcohol to benzaldehyde in comparison with HPW/MIL-101(Cr) (Table 1, entry 5). Further tests were carried out to determine the effect of DAIL groups on the catalytic properties of the PW/DAIL/MIL-101(Cr) catalyst. Therefore, various amounts of DAIL were loaded onto the material. By increasing the loading of DAIL from 0.3 mmol g^{-1} to 0.9 mmol g^{-1}, the conversion increased (Table 1, entries 1–3). Based on these data, it can be concluded that the presence of DAIL groups within the framework of MIL-101(Cr) has a positive effect on the catalytic efficiency. The hydrophilic amino-functionalized IL moiety in the framework, especially the remaining free amino groups anchored on the imidazolium, plays a crucial role in achieving excellent catalytic activity by enhancing the accessibility of TBHP. Within this context, Yang *et al.* reported the efficient epoxidation of *cis*-cyclooctene over a vanadium catalyst using TBHP as the oxidant in the presence of 1-ethyl-3-methylimidazolium bis(trifluoromethylsulfonyl)imide as a co-solvent.[48] The superior catalytic activity of this IL-involved catalytic system was attributed to the hydrogen bonding between the IL and the by-product *t*-butanol, which prevents the coordination of *t*-butanol with the vanadium centre and hence improves the catalytic efficiency. So, the combination of ILs and the catalytically active centres in these catalysts can promote better catalytic efficiency by enhancing the accessibility of oxidants through hydrogen bonding. Additional DAIL groups loaded into the framework resulted in a reduced catalytic activity which may be due to diffusion limitations

Table 1 Catalytic performance of various catalysts in the oxidation of benzyl alcohol

Entry	Catalyst	DAIL loading (mmol g^{-1})	Oxidant/solvent	Conversion[a] (%)	TON[b]
1	PW/DAIL/MIL-101(Cr)	0.3	TBHP/$CHCl_3$	78	1560
2	PW/DAIL/MIL-101(Cr)	0.6	TBHP/$CHCl_3$	85	1700
3	PW/DAIL/MIL-101(Cr)	0.9	TBHP/$CHCl_3$	95	1900
4	PW/DAIL/MIL-101(Cr)	1.5	TBHP/$CHCl_3$	58	1160
5	HPW/MIL-101(Cr)	—	TBHP/$CHCl_3$	70	1400
6	PW/DAIL/MIL-101(Cr)	0.9	TBHP/CH_2Cl_2	81	1620
7	PW/DAIL/MIL-101(Cr)	0.9	TBHP/CH_3CN	65	1300
8	PW/DAIL/MIL-101(Cr)	0.9	H_2O_2/CH_3CN	19	380
9	PW/DAIL/MIL-101(Cr)	0.9	H_2O_2/$CHCl_3$	9	180
10	—	—	TBHP/$CHCl_3$	22	—
11	MIL-101(Cr)	—	TBHP/$CHCl_3$	43	—
12	DAIL/MIL-101(Cr)	0.9	TBHP/$CHCl_3$	47	—
13	HPW	—	TBHP/$CHCl_3$	59	—
14	DAIL[c]	—	TBHP/$CHCl_3$	25	—
15	SiW/DAIL/MIL-101(Cr)	0.9	TBHP/$CHCl_3$	71	1420
16	PMo/DAIL/MIL-101(Cr)	0.9	TBHP/$CHCl_3$	56	1120

Benzyl alcohol (1 mmol), oxidant (4.5 mmol), solvent (1 ml), dodecane (0.5 mmol), catalyst (6 μmol based on W or Mo, 0.5 μmol based on PW, SiW or PMo), time (6 h), 100 °C. [a] GC yield based on the starting substrate. [b] Calculated as mmol of the product formed per mmol of polyoxometalate (PW, SiW or PMo) in the catalyst, selectivity towards the formation of benzaldehyde >99% (determined by GC, entries 1–16). [c] 0.23 mmol DAIL was used as the catalyst.

(Table 1, entry 4). Further tests were carried out to determine the influence of the solvent on the catalytic properties of PW/DAIL/MIL-101(Cr). Higher reactivity of the substrate was obtained in chloroform compared with dichloromethane and acetonitrile. In addition, the PW/DAIL/MIL-101(Cr) catalyst also exhibited higher catalytic activity when TBHP was used as the oxidant. A very low conversion is observed in the absence of the catalyst (22%, Table 1, entry 10).

To clarify the catalytic role of the prepared PW/DAIL/MIL-101(Cr) catalyst, the oxidation reaction was also carried out using the unmodified MIL-101(Cr) and DAIL/MIL-101(Cr) as catalysts. MIL-101(Cr) with unsaturated metal centers at the nodes showed 43% conversion of the benzyl alcohol to benzaldehyde. When DAIL/MIL-101(Cr) was applied as the catalyst, the conversion of benzyl alcohol is slightly higher than that of pristine MIL-101(Cr) (Table 1, entry 12). Moreover, the catalytic performances of the HPW and DAIL were evaluated in the selective oxidation of benzyl alcohol to benzaldehyde, and the results are summarized in Table 1. It is found that the various catalysts of PW/DAIL/MIL-101(Cr) were much more active than the Keggin-type HPW (Table 1, entries 1–3 *cf.* 13), which proves the proficiency of DAIL/MIL-101(Cr) in loading the PW anions.

The comparative data for the selective oxidation of benzyl alcohol over the present catalyst and reported POM-based catalysts are given in Table 2. Patel *et al.* reported the selective aerobic oxidation of benzyl alcohol to benzaldehyde catalyzed by $PMo_{11}Co$.[49] 28–33% conversion of benzyl alcohol was obtained with 92–93% selectivity for benzaldehyde using TBHP as an initiator. Although a very high TON (3628–4281) was achieved, the catalyst gives a relatively low conversion and requires long reaction times (24 h). Later, Wang *et al.* developed a new recyclable amino-functionalized bipyridine–heteropolyacid ionic hybrid, and 100% conversion was observed with 93% selectivity for benzaldehyde.[50] Alternatively, attempts have been made to synthesize supported POM-based IL materials as well. This is another efficient way to fine-tune the surface properties of the support and transfer the ILs' properties to the material. Mesoporous silica and magnetic nanoparticles have been applied as the solid supports, and the results are shown in Table 2.[37,40,51,52] Although high catalytic activity and selectivity were achieved in all the cases, in most reports no turnover number (TON) or turnover frequency (TOF) values were stated. The superiority of our catalysts lies in obtaining *high selectivity towards benzaldehyde with an excellent TON*. Moreover, higher thermal stability is obtained compared to those prepared by the immobilization of POM-based ILs onto mesoporous silica,[40,51,52] which may be attributed to the high stability of MIL-101(Cr) as the solid support.

Catalytic oxidation of benzyl alcohol was carried out in the presence of different POMs. Within this context, $H_4SiW_{12}O_{40}$ and $H_3PMo_{12}O_{40}$ were also immobilized onto DAIL/MIL-101(Cr) to give SiW/DAIL/MIL-101(Cr) and PMo/DAIL/MIL-101(Cr), respectively. The catalytic results in Table 1 clearly show that PW/DAIL/MIL-101(Cr) is the most active catalyst in terms of benzyl alcohol conversion (Table 1, entry 3 *cf.* 15–16). PMo/DAIL/MIL-101(Cr) showed a much lower catalytic performance in the oxidation of benzyl alcohol. This difference in reactivity might be due to the different acidic strengths of the prepared catalysts and the oxidation potentials of their metal centers.

With the aim of examining the catalytic potential of PW/DAIL/MIL-101(Cr) towards other alcohols, various aromatic electron-donating and electron-withdrawing alcohols were examined. The obtained results are listed in Table 3. For aromatic alcohols, the nature of substituents (electron-withdrawing or electron-donating) has a significant effect on aldehyde formation. For example, a high conversion (78%) of 4-methoxybenzyl alcohol into its corresponding aldehyde was observed after 4 h, while for 4-chlorobenzyl alcohol only 45% of its corresponding aldehyde was produced after 6 h.

3.4. Stability and reusability tests

In order to investigate the heterogeneous nature of the PW/DAIL/MIL-101(Cr) catalyst, a hot filtration test was conducted to analyse the existence of the active PW species in solution. Hence, the reaction mixture was filtered after 4 h reaction, and the filtrate was left to react for a further 8 h. The benzyl alcohol conversion reached 80% after 8 h, suggesting that the oxidation reaction does not proceed after the removal of the catalyst (Fig. 7). Additionally, to evaluate the recyclability and reusability of the PW/DAIL/MIL-101(Cr) catalyst, we

Table 2 Comparison of the catalytic activities for the oxidation of benzyl alcohol with reported catalysts

Entry	Catalyst	Reaction conditions	Conversion	Selectivity	Ref.
1	$PMo_{11}M$ (M = Co, Mn, Ni)	Alcohol (100 mmol), catalyst (25 mg), O_2, TBHP (0.2%), 90 °C, 24 h.	28–33	92–93	49
2	DPyAM(H)-PW	Alcohol (10 mmol), catalyst (0.1 g), H_2O_2 (6 mmol), 90 °C, 0.5 h.	100	93.2	50
3	$PV_2Mo_{10}O_{40}$/IL/SMNP	Alcohol (2 mmol), catalyst (1 mmol), 2 atm O_2, 80 °C, 5 h.	98	—	37
4	$PV_2Mo_{10}O_{40}$/IL/SBA15	Alcohol (1 mmol), catalyst (100 mg), air (3.4 atm), 100 °C, 12 h.	98[a]	—	51
5	PW-NH_2-IL-SBA-15	Alcohol (10 mmol), catalyst (0.1 g), H_2O_2 (30 mmol), 100 °C, 6 h.	92	91	52
6	HPW-IL-PMO-15/5m	Alcohol (5 mmol), catalyst (0.1 g), H_2O_2 (15 mmol), 100 °C, 6 h.	88	>99	40
7	HPW-IL-SBA-15/5m	Alcohol (5 mmol), catalyst (0.1 g), H_2O_2 (15 mmol), 100 °C, 6 h.	93	>99	40
8	PW/DAIL/MIL-101(Cr)	Alcohol (1 mmol), catalyst (6 μmol based on W), TBHP (4.5 mmol), 100 °C, 6 h.	95	>99	This work

[a] Based on the GC yield.

Table 3 Catalytic performance of PW/DAIL/MIL-101(Cr) in the oxidation of various alcohols

Entry	Catalyst[a]	Substrate	Time (h)	Conversion[b] (%)	TON[c]
1	PW/DAIL/MIL-101(Cr)	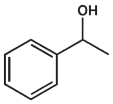	4	100	2000
2	PW/DAIL/MIL-101(Cr)	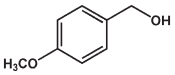	4	78	1560
3	PW/DAIL/MIL-101(Cr)	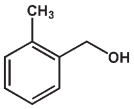	6	59	1180
4	PW/DAIL/MIL-101(Cr)	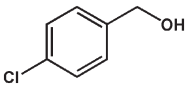	6	45	900

Reaction conditions: aromatic alcohol (1 mmol), TBHP (4.5 mmol), $CHCl_3$ (1 ml), dodecane (0.5 mmol), catalyst (6 μmol based on W, 0.5 μmol based on PW), 100 °C. [a] 0.9 mmol DAIL was used for the preparation of the catalyst. [b] GC yield based on the starting substrate. [c] Calculated as mmol of the product formed per mmol of polyoxometalate (PW) in the catalyst, selectivity towards the formation of benzaldehyde >99% (determined by GC, entries 1–4).

performed the oxidation reaction of benzyl alcohol under the optimized reaction conditions. After reaction completion, the mixture was filtered, and the recycled catalyst was washed with chloroform and acetone. The results presented in Fig. 8 indicate that the catalyst can be recycled and reused up to five times with no significant decrease in catalytic activity. From this, one can conclude that there is little leaching or deactivation of the active components, owing to the strong interaction between the PW and the DAIL/MIL-101(Cr) support. In addition, the filtrate obtained after the recovery of the catalyst was characterized by utilizing the ICP-OES technique to verify if tungsten leaching occurred. The results showed no significant tungsten content in the filtrate during five successive runs (0.00021 wt%).

Further evidence of the high stability of the catalyst was confirmed by DRIFT and PXRD analyses. The results from the DRIFT characterization of the recycled PW/DAIL/MIL-101(Cr) catalyst (see the ESI,† Fig. S5) show all the characteristic peaks of the DAIL and PW molecules, suggesting that the main structure of the catalyst is preserved. The similarity of the PXRD patterns of PW/DAIL/MIL-101(Cr) before catalysis and after each run clearly suggests the high stability of the structure under reaction conditions (see the ESI,† Fig. S6).

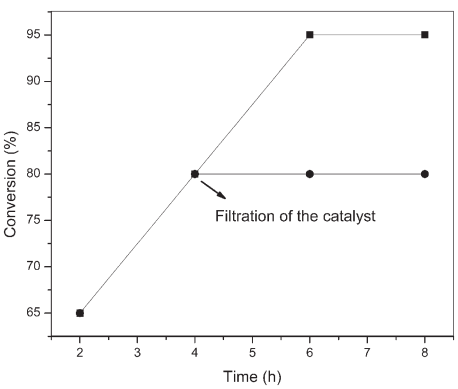

Fig. 7 Hot filtration test for the PW/DAIL/MIL-101(Cr) catalyst.

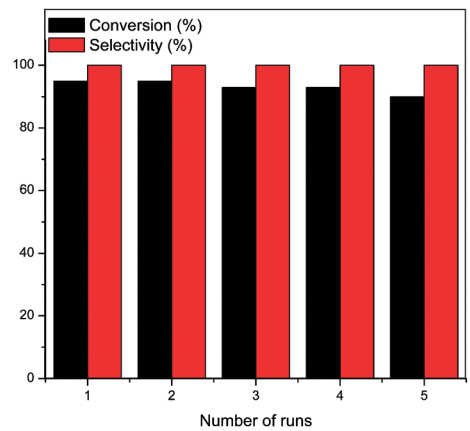

Fig. 8 Recyclability of the PW/DAIL/MIL-101(Cr) catalyst.

4 Conclusions

In summary, we have designed and synthesized a new, environmentally-friendly POM-based catalyst using dual amino-functionalized basic ionic liquid (DAIL)-modified MIL-101(Cr) as a solid support. The good thermal stability and also the presence of two primary amine groups, in which the free amino group is able to form hydrogen bonds, make the DAIL a good candidate to be immobilized onto MIL-101(Cr). This proved to be a successful and efficient approach to increase the catalytic activity of the resulting catalyst. The catalyst enables the oxidation of benzyl alcohol with complete selectivity towards benzaldehyde. The PW/DAIL/MIL-101(Cr) catalyst can be recovered and reused at least five times with no significant loss in activity. Moreover, the combination of

MIL-101(Cr), DAIL and HPW resulted in a heterogeneous catalyst with enhanced thermal stability and Langmuir surface area compared to those prepared by the immobilization of POM-based ILs onto mesoporous silica.

This work is an important step towards the heterogenization of ionic liquids to design heterogeneous POM-based ionic liquids.

Acknowledgements

Sara Abednatanzi gratefully acknowledges financial support from the University of Tehran. Karen Leus acknowledges financial support from the Ghent University BOF-post-doctoral Grant 01P06813T.

References

1 R. A. Sheldon, I. W. C. E. Arends and A. Dijksman, *Catal. Today*, 2000, **57**, 157.
2 C. Bai, A. Li, X. Yao, H. Liu and Y. Li, *Green Chem.*, 2016, **18**, 1061.
3 H. Miyamura, R. Matsubara, Y. Miyazaki and S. Kobayashi, *Angew. Chem., Int. Ed.*, 2007, **46**, 4151.
4 D. I. Enache, J. K. Edwards, P. Landon, B. Solsona-Espriu, A. F. Carley, A. A. Herzing, M. Watanabe, C. J. Kiely, D. W. Knight and G. J. Hutchings, *Science*, 2006, **311**, 362.
5 J. E. Backvall, *Modern Oxidation Methods*, Wiley-VCH Verlag, 2nd edn, 2010.
6 M. Sankar, E. Nowicka, E. Carter, D. M. Murphy, D. W. Knight, D. Bethell and G. J. Hutchings, *Nat. Commun.*, 2014, **5**, 3332.
7 C. L. Hill and C. M. Prosser-McCartha, *Coord. Chem. Rev.*, 1995, **143**, 407.
8 N. Mizuno and M. Misino, *Chem. Rev.*, 1998, **98**, 199.
9 R. Neumann, *Prog. Inorg. Chem.*, 1998, **47**, 317.
10 N. Mizuno, K. Yamaguchi and K. Kamata, *Coord. Chem. Rev.*, 2005, **249**, 1944.
11 Y. Leng, W. Zhang, J. Wang and P. Jiang, *Appl. Catal., A*, 2012, **445-446**, 306.
12 G. Chen, Y. Zhou, Z. Long, X. Wang, J. Li and J. Wang, *ACS Appl. Mater. Interfaces*, 2014, **6**, 4438.
13 E. Rafiee and S. Eavani, *J. Mol. Catal.*, 2014, **199**, 96.
14 M. Y. Huang, X. X. Han, C. T. Hung, J. C. Lin, P. H. Wu, J. C. Wu and S. B. Liu, *J. Catal.*, 2014, **320**, 42.
15 S. S. Wang, W. Liu, Q. X. Wan and Y. Liu, *Green Chem.*, 2009, **11**, 1589.
16 N. M. Okun, T. M. Anderson and C. L. Hill, *J. Am. Chem. Soc.*, 2003, **125**, 3194.
17 M. V. Vasylyev and R. Neumann, *J. Am. Chem. Soc.*, 2004, **126**, 884.
18 J. J. Alcañiz, J. Gascon and F. Kapteijn, *J. Mater. Chem.*, 2012, **22**, 10102.
19 K. Yamaguchi, C. Yoshida, S. Uchida and N. Mizuno, *J. Am. Chem. Soc.*, 2005, **127**, 530.
20 J. J. Alcañiz, J. Gascon and F. Kapteijn, *J. Mater. Chem.*, 2012, **22**, 10102.
21 A. Dhakshinamoorthy, M. Opanasenko, J. Čejka and H. Garcia, *Catal. Sci. Technol.*, 2013, **3**, 2509.
22 K. K. Tanabe and S. M. Cohen, *Inorg. Chem.*, 2010, **49**, 6766.
23 S. Abednatanzi, P. Gohari Derakhshandeh, A. Abbasi, P. Van Der Voort and K. Leus, *ChemCatChem*, 2016, **8**, 3672.
24 S. Abednatanzi, A. Abbasi and M. Masteri-Farahani, *New J. Chem.*, 2015, **39**, 5322.
25 K. Leus, Y. Y. Liu, M. Meledina, S. Turner, G. Van Tendeloo and P. Van Der Voort, *J. Catal.*, 2014, **316**, 201.
26 Y. Y. Liu, K. Leus, T. Bogaerts, K. Hemelsoet, E. Bruneel, V. Van Speybroeck and P. Van Der Voort, *ChemCatChem*, 2013, **5**, 3657.
27 S. Abednatanzi, A. Abbasi and M. Masteri-Farahani, *J. Mol. Catal. A: Chem.*, 2015, **399**, 10.
28 D. Jiang, L. L. Keenan, A. D. Burrows and K. J. Edler, *Chem. Commun.*, 2012, **48**, 12053.
29 Z. Sun, G. Li, H. O. Liu and L. Liu, *Appl. Catal., A*, 2013, **466**, 98.
30 R. Canioni, C. Roch-Marchal, F. Sécheresse, P. Horcajada, C. Serre, M. Hardi-Dan, G. Férey, J.-M. Grenèche, F. Lefebvre, J.-S. Chang, Y.-K. Hwang, O. Lebedev, S. Turnerf and G. Van Tendeloo, *J. Mater. Chem.*, 2011, **21**, 1226.
31 D. M. Fernandes, A. D. S. Barbosa, J. Pires, S. S. Balula, L. Cunha-Silva and C. Freire, *ACS Appl. Mater. Interfaces*, 2013, **5**, 13382.
32 L. Bromberg, Y. Diao, H. Wu, S. A. Speakman and T. A. Hatton, *Chem. Mater.*, 2012, **24**, 1664.
33 J. T. Hupp and K. R. Poeppelmeier, *Science*, 2005, **309**, 2008.
34 S. Bhattacharjee, C. Chen and W.-S. Ahn, *RSC Adv.*, 2014, **4**, 52500.
35 Y. Chen and Y. F. Song, *ChemPlusChem*, 2014, **79**, 304.
36 Y. Leng, J. Zhao, P. Jiang and J. Wang, *ACS Appl. Mater. Interfaces*, 2014, **6**, 5947.
37 J. Zhu, P. Ch. Wang and M. Lu, *RSC Adv.*, 2012, **2**, 8265.
38 K. Yamaguchi, Ch. Yoshida, S. Uchida and N. Mizuno, *J. Am. Chem. Soc.*, 2005, **127**, 530.
39 M. Bagheri, M. Masteri-Farahani and M. Ghorbani, *J. Magn. Magn. Mater.*, 2013, **327**, 58.
40 H. Zhao, L. Zeng, Y. Li, Ch. Liu, B. Hou, D. Wu, N. Feng, A. Zheng, X. Xie, Su Sh and N. Yu, *Microporous Mesoporous Mater.*, 2013, **172**, 67.
41 H. Wan, Ch. Chen, Z. Wu, Y. Que, Y. Feng, W. Wang, L. Wang, G. Guan and X. Liu, *ChemCatChem*, 2015, **7**, 441.
42 J. Zhang, C. Jia, H. Dong, J. Wang, X. Zhang and S. Zhang, *Ind. Eng. Chem. Res.*, 2013, **52**, 5835.
43 D. M. Jiang, A. D. Burrows and K. J. Edler, *CrystEngComm*, 2011, **13**, 6916.
44 D. Julião, A. C. Gomes, M. Pillinger, L. Cunha-Silva, B. de Castro, I. S. Gonçalves and S. S. Balula, *Fuel Process. Technol.*, 2015, **131**, 78.
45 M. Saikia, D. Bhuyan and L. Saikia, *New J. Chem.*, 2015, **36**, 64.
46 Q.-X. Luo, X.-D. Song, M. Ji, S.-E. Park, C. Hao and Y.-Q. Li, *Appl. Catal., A*, 2014, **478**, 81.
47 K. R. Seddon and A. Stark, *Green Chem.*, 2002, **4**, 119.

48 L. Bai, K. Li, Y. Yan, X. Jia, J.-M. Lee and Y. Yang, *ACS Sustainable Chem. Eng.*, 2016, **4**(2), 437.
49 S. Pathan and A. Patel, *Catal. Sci. Technol.*, 2014, **4**, 648.
50 Y. Leng, P. Zhao, M. Zhang and J. Wang, *J. Mol. Catal. A: Chem.*, 2012, **358**, 67.
51 A. Bordoloi, S. Sahoo, F. Lefebvre and S. B. Halligudi, *J. Catal.*, 2008, **259**, 232.
52 R. Tan, C. Liu, N. Feng, J. Xiao, W. Zheng, A. Zheng and D. Yin, *Microporous Mesoporous Mater.*, 2012, **158**, 77.